



Indian Journal of Engineering & Materials Sciences
Vol. 27, June 2020, pp. 529-537



A band-selective CMOS low-noise amplifier with current reuse g_m boosting technique for 3-5 GHz UWB receivers

Jaemin Shim^a, Jinwoopark^b & Jichai Jeong^{b*}

^aDepartment of Computer and Radio Communication Engineering, Korea University, 145, Anam-ro, Sungbuk-ku, Seoul 02841, Korea

^bDepartment of Brain and Cognitive Engineering, Korea University, 145, Anam-ro, Sungbuk-ku, Seoul 20841, Korea

Received: 21 October 2015 ; Accepted: 29 August 2017

The authors have proposed a 3-5 GHz ultra-wideband (UWB) low power and low noise amplifier (LNA) with the TSMC 0.18 μm RF CMOS process, which uses a novel dual input matching network for wideband matching. We have used a current-reuse g_m -boosted common-gate topology and shunt-shunt feedback common-source output buffer to improve gain and noise figure with low power dissipation. The proposed dual input matching g_m -boosted common-gate LNA has been efficient bandwidth to cover UWB band. It has required less inductors or amplification stages to increase bandwidth as compared with the conventional UWB common-gate LNAs. The broadband input stage has been able to be switched to three frequency bands with capacitive switches. The capacitive switch has replaced a large inductor to resonate at lower frequency band. The band-selective LNA has shown linearity improvement by attenuating the undesired interference of a wideband gain circuit and using less inductors. Simulated performance has shown the gains of 15.9, 17.6, and 16.9 dB, and the noise figures of 3.38, 3.28, and 3.27 dB at the 3.432, 3.960, and 4.488 GHz frequency bands, respectively. The proposed UWB LNA has consumed 5 mW from a 1.8-V power supply.

Keywords: CMOS, UWB, Low noise amplifier, g_m -boosted common-gate amplifier, Current-reuse technique, Dual input matching, Band-selective switching capacitor

1 Introduction

In recent years, ultra-wideband (UWB) systems have emerged as a new wireless communication technology capable of high data transmission rates with low power. Since the Federal Communications Commission (FCC) released the UWB radios frequency spectral mask in 2002, the IEEE 802.15.6 standard for short-range and low-power wireless communications has been defined by the IEEE LAN/MAN standards committee in 2012. It is targeted at applications such as wireless body area networks (WBAN) operated in the vicinity of a human body. For UWB low-noise amplifiers (LNA), we have to consider performance parameters such as sufficient flat gain, wideband input and output return loss, low noise figures, low power dissipation for mobility, good linearity, and small chip area for low cost.

LNA can determine the frequency range of the entire receiver. There have been many approaches to wideband operation. The simplest way to receive a wide frequency band is a distributed amplifier providing sufficient input/output matching conditions

and good linearity¹⁻³. However, this has some problems, with high power consumption to operate multi-amplifying stages and occupies a significant chip area, resulting in high cost for integration. There are also wideband LNA design techniques using resistive feedback⁴⁻⁸. However, the feedback resistor tends to degrade the noise performance of the LNA. A wideband amplifier can also be designed with a passive LC filter providing wide input matching⁹⁻¹¹, but this needs some inductors that require a large die area. The common-gate topology is an alternative way of providing wide input matching due to the constant wide input impedance (of $1/g_m$)^{12,13}. Although the noise factor of a common-gate LNA is slightly higher than common-source LNA, it remains almost constant regardless of the frequency operation and bandwidth. The g_m -boosting technique can reduce the output noise floor of a common-gate LNA¹⁴. However, the g_m -boosted common-gate amplifier is still insufficient to cover UWB band. To cover UWB band, the conventional common-gate amplifiers use additional inductors or amplification stages to enhance the wideband performance and gain flatness¹⁵⁻¹⁷. But the additional inductors degrade the linearity and noise figure, and need large die area. The supplementary

*Corresponding author (E-mail: jcj@korea.ac.kr)

amplification stage also has a disadvantage of high power consumption. To improve the performance deficiencies of the conventional amplifier, we employ a dual input matching network using only its own amplification structure without additional devices. However, the broadband gain response requires high power consumption to cover broad frequency bands with sufficient gain and does not attenuate undesired interference. In this paper, we propose a band-selective amplifier with switches to amplify a divided narrow frequency band with lower power dissipation and higher gain than a broad frequency band and attenuate interference¹⁸⁻²¹. To minimize the use of large size inductors, we use capacitive switches. The proposed LNA can be switched to three frequency bands, such as the 3.432, 3.960, and 4.488 GHz bands. A current-reuse structure is also implemented to save power consumption in a cascaded common-gate and common-source stage¹⁵. To achieve higher gain without additional power consumption, we modified the output buffer to a common-source stage with a RC feedback topology²².

2 Design of Proposed Band-Selective UWB LNA

A schematic diagram of the proposed UWB LNA is shown in Fig. 1. The first stage is the wideband g_m -boosted common-gate amplifier for low power consumption¹⁴. It consists of capacitive switches for band selection¹⁸⁻²¹. The second stage is the resistive feedback common-source buffer providing sufficient

gain and output matching²². In this section, the design concepts of the LNA are followed by a detailed description.

2.1 g_m -Boosted Common-Gate UWB LNA with Current-Reuse Technique

The basic common-gate amplifier topology benefits include wideband input matching of $1/g_m$, although it provides poorer noise performance than a common-source amplifier at low operating frequencies^{12,13}. The g_m -boosting technique can improve the noise figure of the common-gate LNA and preserve its advantages of linearity, stability, and low power dissipation by applying the signal on both the gate and source simultaneously¹⁴.

Conventionally, the g_m -boosting technique is popular with the capacitor cross-coupling technique in a differential structure. The capacitor cross-coupling technique enables the g_m -boosting effect with no DC power cost. However, the capacitor cross-coupling technique limits boosting gain to less than 1, because it is based on passive amplification¹⁴. The transformer of the input stage provides g_m -boosting gain²³. Because the passive device transformer consumes no power, it is suitable for low-power circuits. However, it is not appropriate for adoption in broadband circuits due to nonlinearities and low parasitic resistance. The auxiliary active amplifier of the inverting gain is the last method of the g_m -boosting technique²⁴, but it requires a high power dissipation budget.

To save power dissipation, current-reuse technique has been proposed¹⁵. Conventionally, current-reuse technique stacks the cascaded common-source stages sharing the bias current. Because the current-reuse technique using a common-source amplifier has a narrow frequency band, the proposed circuit is based on cascaded common-gate and common-source (CG-CS) stages for wide input matching. The common-source stage is also biased separately, leading to higher power consumption. To improve power performance, the proposed LNA stacked the MOS common-source stage on the common-gate stage¹⁶. The stacked CG-CS stages share the same bias current. Then, the proposed circuit reduces the power dissipation associated with the g_m -boosting method. Although the common-gate amplifier has broad input matching, it is ineffective to cover UWB band. Therefore, the conventional common-gate wideband amplifiers adopt band pass filter, peaking inductor, or cascade amplifier to reinforce the bandwidth of common-gate amplifier. However, the

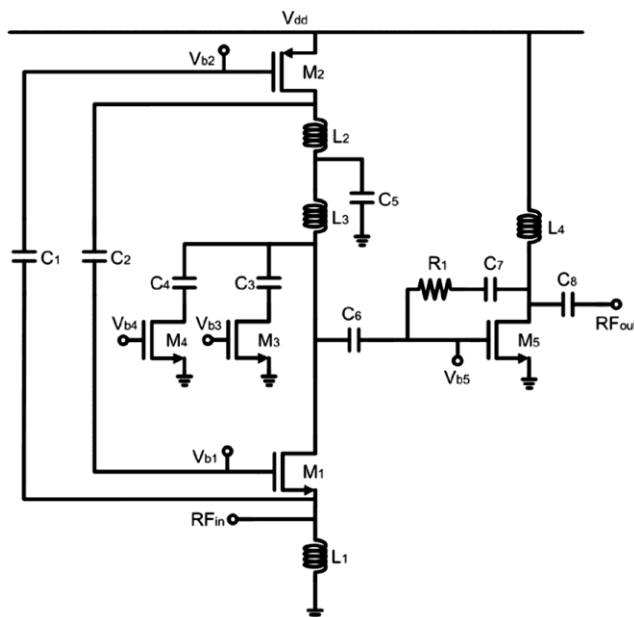


Fig. 1 — Circuit diagram of the proposed band-selective UWB LNA.

additional inductors and amplification stages degrade linearity and noise figure, and increase chip area and power dissipation. To improve the performance of the conventional common-gate circuit, we implement a dual input matching network using adopted current-reused g_m -boosting stage without additional elements.

Figure 2 shows a schematic of the input stage of the proposed LNA. The input impedance Z_{in} can be expressed as:

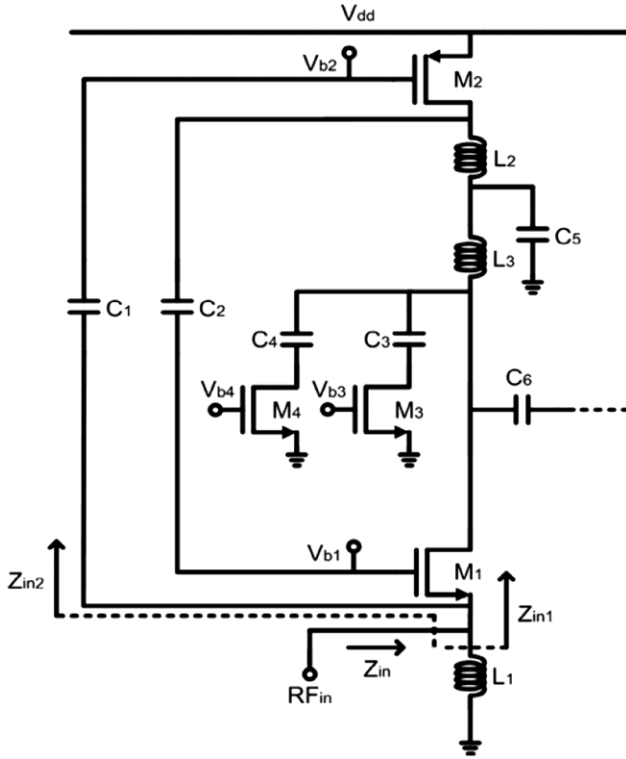


Fig. 2 — Schematic of input stage network for wideband input impedance matching with the common-gate and common-source stages.

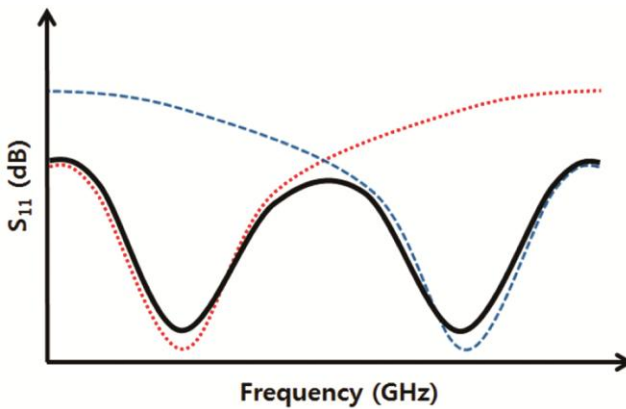


Fig. 3 — Principle of wide band input matching characteristic combining the lower frequency band and upper frequency band input matching.

$$Z_{in} = Z_{in1} // Z_{in2} \quad \dots (1)$$

Z_{in1} is the input impedance of the LNA when the effect of the g_m -boosting stage is ignored. Z_{in2} is the impedance looking into the g_m -boosting common-source stage. Thus, we can have each resonant frequency $\omega_{o,in1}$ of the common-gate stage and $\omega_{o,in2}$ of the g_m -boosting stage. If the resonant frequencies $\omega_{o,in1}$ and $\omega_{o,in2}$ are not too close, the LNA circuit has two input matching points²⁵. The input reflection coefficients (S_{11}) are notch functions at frequencies $\omega_{o,in1}$ and $\omega_{o,in2}$, as shown in Fig. 3. The overlapped S_{11} of two input matching points can be considered as a broad input matching. Figure 3 shows the overall input reflection coefficient with combination of the lower frequency band ($\omega_{o,in1}$) and upper frequency band ($\omega_{o,in2}$) input matching. The common-gate stage is used for lower frequency band input matching. The upper frequency band input matching consists of common-source stage. Thus, the proposed LNA can be matched to a wide input frequency band.

Figure 4 shows the equivalent small-signal model of the proposed g_m -boosted common gate UWB LNA with a current-reuse technique excluding the output stage¹⁶. v_{in} is the small signal input source, R_s is the source resistance, C_{gs1} and C_{gs2} are the gate-to-source capacitances of M_1 and M_2 , v_{gs1} and v_{gs2} are the gate-to-source small signal voltages of the respective MOS, respectively. g_{m1} and g_{m2} are the transconductances of M_1 and M_2 , respectively. r_{ds1} and r_{ds2} are the short channel resistances of M_1 and M_2 , respectively. To simplify the analysis, the large ac-coupling capacitors C_1 and C_2 are replaced by short circuits. Similarly, the large bypass capacitor C_5 is also replaced by a short circuit. The g_m -boosting gain $A_{g_m\text{-boosting}}$ can be approximated by¹⁶

$$A_{g_m\text{-boosting}}(\omega) \approx -g_{m2} \cdot (r_{ds2} // j\omega L_2) \quad \dots (2)$$

The overall gain A_1 of the first stage of the proposed UWB LNA is given by

$$A_1(\omega) = \frac{\{1 + (1 + A_{g_m\text{-boosting}}) \cdot g_{m1} r_{ds1}\} j X_n}{R_s \cdot \{1 + (1 + A_{g_m\text{-boosting}}) \cdot g_{m1} r_{ds1} + j B_1 \cdot (r_{ds1} + j X) \} + (r_{ds1} + j X)} \quad \dots (3)$$

The reactance X_n has three different values by band selection switches. Figure 5 shows the equivalent circuit model in the on and off modes of the switched capacitors. $C_{3,4}$ are the switch capacitors,

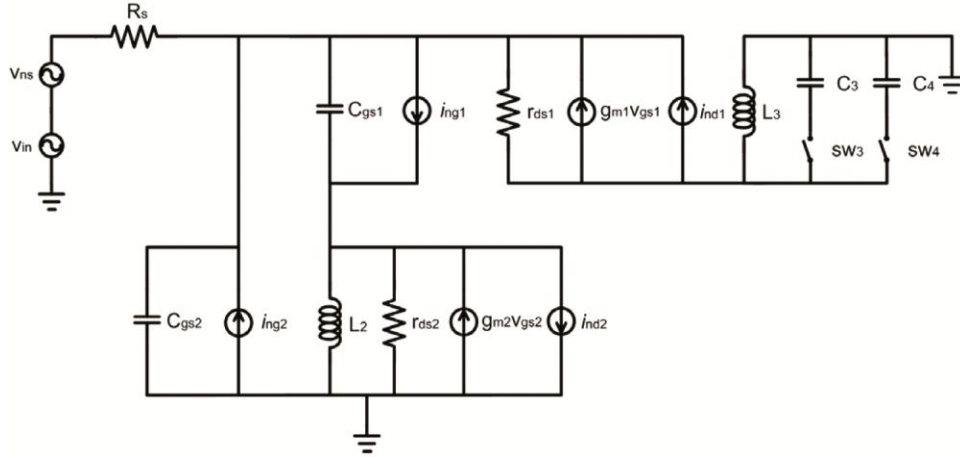


Fig. 4 — Small-signal equivalent model of the proposed band-selective UWB LNA with relevant noise sources.

$R_{on3,4}$ are the on-resistances of the transistor switches, $C_{p3,4}$ are the parasitic capacitance of the transistor switches. The transistor switches $M_{3,4}$ need to have low resistance and parasitic capacitance to optimize the characteristics of a circuit. Increasing the transistor switch size reduces the resistance, resulting in also increasing the parasitic capacitance. Therefore, the widths of the transistor switches $M_{3,4}$ are determined to $25\mu\text{m}$ by considering the trade-off relation between resistance and capacitance. The capacitor sizes of $C_{3,4}$ are determined by target resonance frequencies of the LNA.

$$X_{n-off}(\omega) = \omega L_3 // \frac{1}{\omega \{(C_3 // C_{p3}) + (C_4 // C_{p4})\}} \quad \dots (4)$$

$$X_{n-onC_3}(\omega) = \omega L_3 // \frac{1}{\omega \{(C_3 + C_{p3}) + (C_4 // C_{p4})\}} \quad \dots (5)$$

$$X_{n-onC_{3,4}}(\omega) = \omega L_3 // \frac{1}{\omega \{(C_3 + C_{p3}) + (C_4 + C_{p4})\}} \quad \dots (6)$$

In Fig. 4, v_{ns} is the noise generator for the source resistance R_s , i_{nd1} and i_{nd2} are the drain current noise sources, and i_{ng1} and i_{ng2} are the corresponding gate current noise sources. The noise factor of the first stage of the proposed UWB LNA is given by:

$$F = \frac{\gamma g_{d01}}{R_s} \left[\frac{r_{ds1}^2}{\{1 + (1 + A_{gm-boosting}) \cdot g_{m1} r_{ds1}\}^2} \right] \times \frac{1}{\{1 + R_s^2 \cdot (B_1 + B_{c1})^2\}} \quad \dots (7)$$

$$+ \frac{\delta B_1^2 R_s}{5 g_{d01}} + \frac{\gamma g_{d02}}{R_s} \beta^2 + \frac{\delta B_2^2 R_s}{5 g_{d02}} + 2 \beta B_2 \sqrt{\frac{\delta \gamma}{5}}$$

$$B_1(\omega) = \{1 + A_{gm-boosting}(\omega)\} \cdot \omega C_{gs1} \quad \dots (8)$$

$$B_2(\omega) = \omega C_{gs2} \quad \dots (9)$$

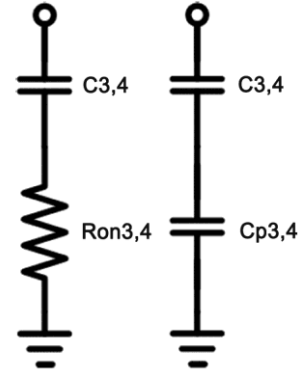


Fig. 5 — Modeling of the switch in on and off modes.

$$B_{c1}(\omega) = \frac{B_1(\omega)}{(1 + A_{gm-boosting})} \left\{ \frac{1 + (1 + A_{gm-boosting}) \cdot g_{m1} r_{ds1}}{r_{ds1} g_{d01}} |c| \sqrt{\frac{\delta}{5\gamma}} \right\} \quad \dots (10)$$

$$\beta(\omega) = \frac{1}{g_{m2}} \sqrt{\frac{[\{1 + (1 + A_{gm-boosting}) \cdot g_{m1} r_{ds1}\} \cdot R_s + r_{ds1} - B_1 R_s X_n]^2 + (X_n + B_1 R_s r_{ds1})^2}{r_{ds1}^2 + X_n^2}} \quad \dots (11)$$

where c is the correlation coefficient, g_{d01} is the zero bias channel conductance, and γ and δ are the bias dependent constants. Whereas the drain current noise of M_1 can be reduced by the g_m -boosting gain, the g_m -boosting gain deteriorates the input referred noise of M_2 . Therefore, the g_m -boosting gain must be set carefully to obtain minimum noise.

2.2 Band Selection by Switching Capacitor

The proposed circuit has a wide tuning range with switched capacitors¹⁸⁻²¹. The broadband response circuit does not attenuate undesired interference and spurious noise. The proposed LNA circuit is band-

selectable to attenuate the broadband noise issue at the tuned operating frequency range. The g_m -boosted common-gate stage performs broadband input matching and amplification. By changing the value of the passive element employing the transistor switched capacitor, the common-source g_m -boosting stage provides wide range frequency tuning while power dissipation remains low. The two switched capacitors provide band selection by the LC resonance tank. The proposed switched LC tank covers the entire frequency range of 3-5 GHz.

Transistors M_3 and M_4 are the switches that change the resonance frequency of the g_m -boosting stage. The selection of frequency bands can be implemented by a switched inductor or capacitor²⁶. Inductive switching needs a large chip area. To reduce die area, we substitute the parallel LC network using capacitive switch for large size inductor to resonate at lower frequency band. In capacitive switching, the additional capacitor can select a lower frequency band, by turning on a corresponding transistor switch. The LC network can be modeled as an inductor and a resistor²⁷. For the frequency range under the resonant frequency of LC circuit, its impedance can be derived as

$$Z = j\omega L + R \quad \dots (12)$$

$$L \approx \frac{L_3}{1 - \omega^2 L_3 C_t} = \frac{L_3}{1 - (\omega/\omega_{01})^2} \quad \dots (13)$$

$$R \approx \frac{R_p}{(1 - \omega^2 L_3 C_t)^2} = \frac{R_p}{(1 - (\omega/\omega_{01})^2)^2} \quad \dots (14)$$

$$C_{t1,off} = (C_3 // C_{p3}) + (C_4 // C_{p4}) \quad \dots (15)$$

$$C_{t1,on C_3} = (C_3 + C_{p3}) + (C_4 // C_{p4}) \quad \dots (16)$$

$$C_{t1,on C_{3,4}} = (C_3 + C_{p3}) + (C_4 + C_{p4}) \quad \dots (17)$$

where R_p is the parasitic resistance, C_{t1} is the total capacitance of the switched capacitor at different switching modes. Large gap frequency band switching needs a large capacitance value. The large integrated capacitors lose high RF signals because of large parasitic capacitance to the substrate and this degrades the overall quality factor of the LC resonance. However, the distances of the interest frequency bands of the proposed LNA are small, resulting in low capacitive switching degradation.

2.3 RC-Feedback Output Buffer

The output stage using a source follower structure can achieve wide band matching with 50Ω impedance, but it cannot increase the LNA gain. Therefore,

RC-feedback common-source stage²² is used to achieve higher gain, as shown in Fig. 6. The common-source buffer with a shunt-shunt feedback can enhance the gain, noise, and bandwidth performances. The output terminal resonance frequency can be determined by choosing the inductance L_4 and capacitance C_8 at output terminal properly, as follows:

$$f = \frac{1}{2\pi} \sqrt{\frac{1}{L_4 C_{t2}}} \quad \dots (18)$$

The R_1 and C_7 compose the shunt-shunt RC-feedback topology, so that the circuit achieves a flat and wide bandwidth. The L_4 and C_{t2} compensate the output resonance frequency. The C_{t2} is the total capacitance including the C_8 and parasitic capacitance. The C_6 matches the first and second stages connection.

Figure 7 represents the equivalent small-signal model of the common-source feedback buffer⁸. g_{m5} is the trans conductance of M_5 , and C_{gs5} is the gate-to-source capacitances of M_5 . The dc blocking capacitors C_6 , C_7 , and C_8 are replaced by short circuits. Using the small-signal model the gain of the common-source buffer can be simplified as⁸:

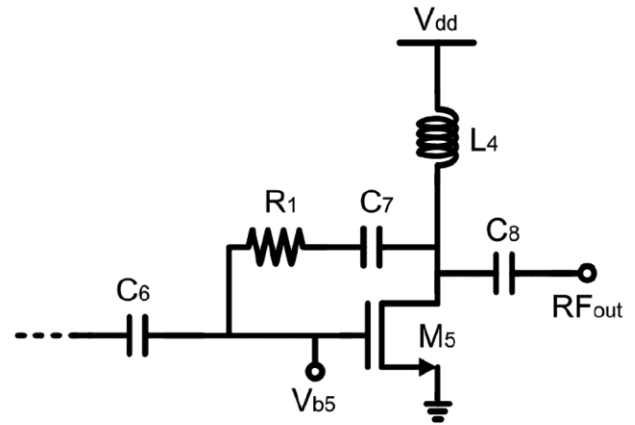


Fig. 6 — Output buffer with the RC-feedback topology to improve gain.

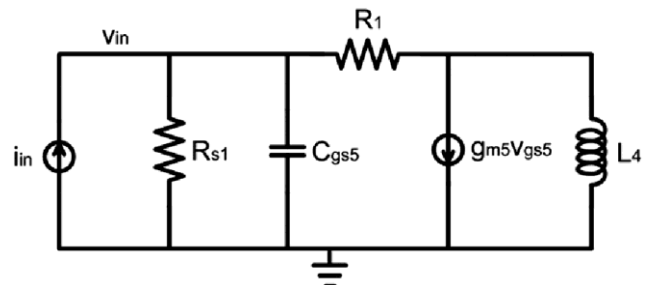


Fig. 7 — Small-signal equivalent model of the RC-feedback output buffer matching.

$$A_{CS} = -(g_{m5} - \frac{1}{R_1}) \cdot (j\omega L_4 // R_1) \quad \dots (19)$$

The feedback reduces the output impedance of the common-source amplifier and achieves wide band output matching. The output impedance of the feedback common-source buffer is given by

$$Z_{out} = \frac{j\omega L_4 // R_1}{1 + g_{m5} \cdot (j\omega L_4 // R_1) \cdot \frac{1}{R_1}} \quad \dots (20)$$

The noise figure of the common-source buffer is calculated by:

$$NF \approx 1 + \frac{\gamma}{R_{S1} \cdot g_{m5}} + \frac{1}{R_{S1} \cdot j\omega L_4 \cdot g_{m5}^2} + \frac{4R_{S1}}{R_1} \left(\frac{-1}{1 + \frac{R_1 + R_{S1}}{(1 + g_{m5} R_{S1}) \cdot j\omega L_4}} \right)^2 \quad \dots (21)$$

The feedback resistance can reduce the noise figure as shown in Eq. (21). The common-source output stage using the RC-feedback topology improves the gain and noise figure.

3 Simulation Results of the Proposed UWB LNA

The proposed band-selective LNA operates at the 3.432, 3.960, and 4.488 GHz frequency bands to cover the 3-5 GHz UWB band. The proposed LNA was implemented with a TSMC 0.18 μm RF CMOS

process using a 1.8-V supply voltage. The proposed circuit uses the current reuse g_m -boosting technique with a switched capacitor and RC feedback output buffer to increase the gain and reduce the power consumption. The S-parameters, noise figure, and IIP3 simulation were performed at a schematic-level using a Cadence RF Spectre.

3.1 Gain

Figure 8 shows the simulated gain of the proposed band-selective amplifier for three different gain modes across the three extreme corners, best case, typical case, and worst case as a function of frequency. The center frequency and bandwidth of each extreme corner case vary due to process, voltage, and temperature variation. The g_m -boosting common-source stage (M_2) increases the LNA gain without additional power consumption by the current-reuse technique. The current-reuse technique modifies a cascade structure to a cascode structure, sharing bias current of common- gate and common-source amplifiers. The feedback common-source output stage (M_5), also increases the gain of the proposed LNA circuit. In each gain mode, gains of 15.9, 17.6, and 16.9 dB were achieved at 3.432, 3.960, and 4.488 GHz, respectively, with 5 mW power dissipation. The two capacitive switching transistors controlling gain are turned on and off according to the three gain modes.

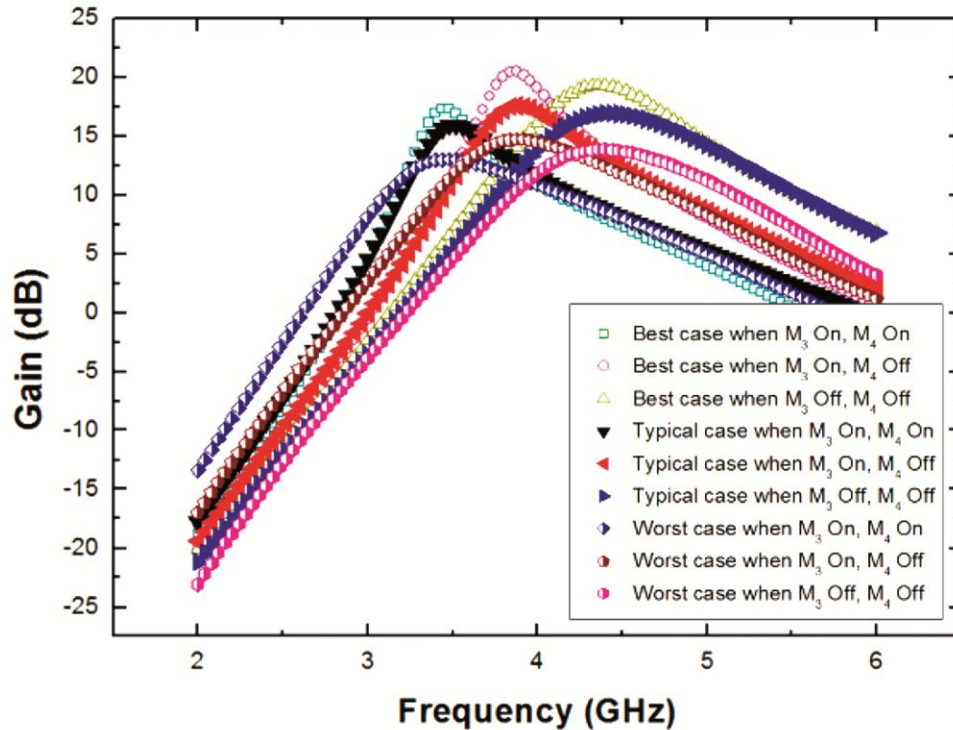


Fig. 8 — Simulated power gain characteristics across the three extreme corners, best case, typical case, and worst case for three different gain modes versus frequency.

3.2 Noise Figures

Figure 9 shows the noise figures simulated at the three different gain modes. Because the g_m -boosting method reduces the noise factor and increases the transconductance, the proposed band-selective LNA has a low noise figure with low power consumption. The minimum noise figures are 3.38, 3.28, and 3.27 dB at 3.432, 3.960, and 4.488 GHz, respectively.

3.3 Input/output Return Loss

The proposed LNA achieves wide input impedance matching with two resonance frequencies of common-gate and common-source stages. Figure 10 shows the input and output return loss over 3-5 GHz. Although the input matching of upper frequency band is affected by switched LC resonance, the input return loss (S_{11}) values are below -10 dB. The output return loss (S_{22}) values of

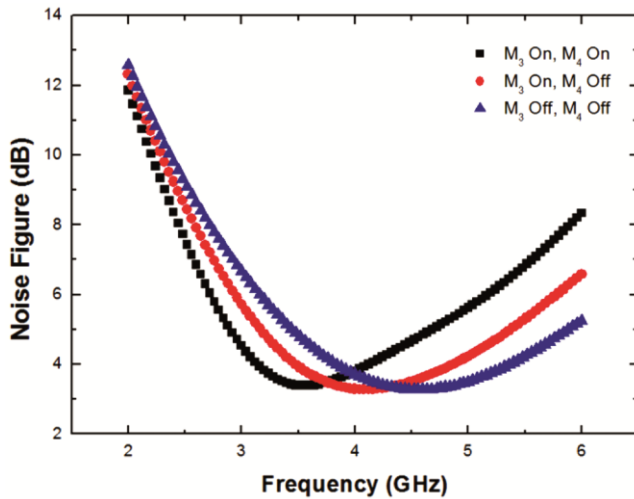


Fig. 9 — Simulated noise figure characteristics versus frequency for the 3.432 GHz, 3.960 GHz, and 4.488 GHz bands.

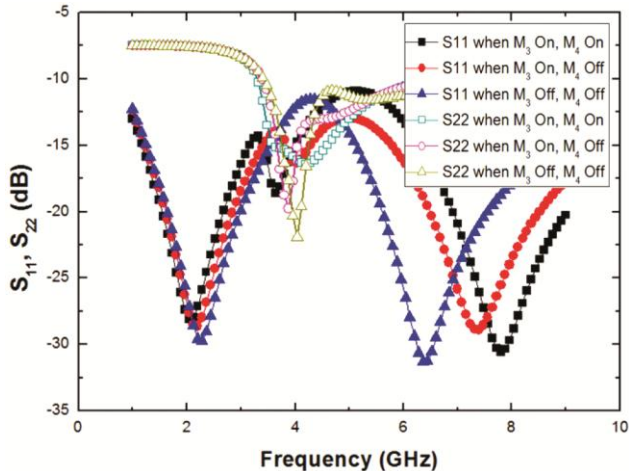


Fig. 10 — Simulated frequency responses of input return loss (S_{11}), and output return loss (S_{22}) as a function of frequency.

LNA satisfy the output matching condition due to RC-feedback output buffer. Even though S_{22} is over -10 dB at lower frequency part of 3.432 GHz frequency band mode, overall S_{22} is below -10 dB. These results indicate the effectiveness of wideband matching.

3.4 Linearity and Stability

The input third-order-intercept points (IIP3) were simulated using a two-tone test with a 10 MHz spacing at 3.432, 3.960, and 4.488 GHz. As shown in Fig. 11, the IIP3 was estimated as -7.1 dBm at 3.432 GHz, -9.3 dBm at 3.960 GHz, and -8.1 dBm at 4.488 GHz. The input power was swept from -40 to 0 dBm. Figure 12 shows the K-factor of the proposed LNA. The UWB LNA satisfies the unconditionally stable conditions over each frequency bands of interest²⁸.

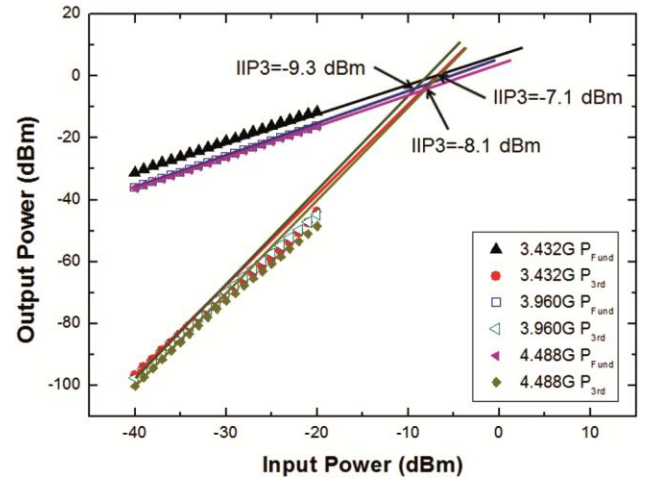


Fig. 11 — Simulated results of IIP3 characteristics at 3.432 GHz, 3.960 GHz, and 4.488 GHz with the two tone test using 10 MHz spacing.

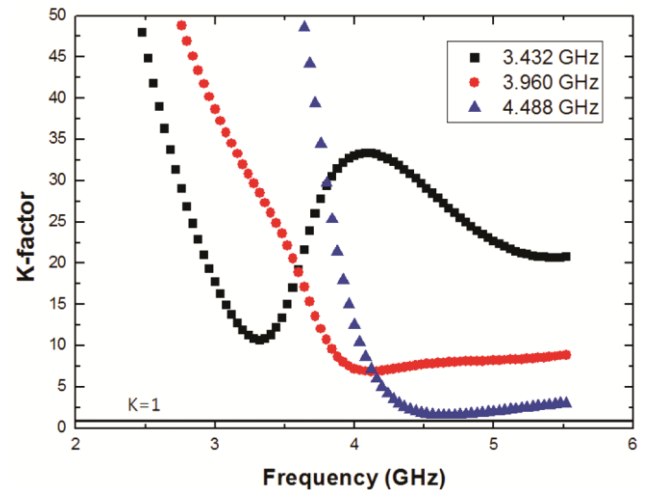


Fig. 12 — K-factor of the proposed UWB LNA versus frequency.

Table 1 — Device sizes and values of the proposed UWB LNA

| | | | | | | | | |
|------------|----------------|----------------|----------------|----------------|----------------|----------------|----------------|----------------|
| Transistor | M ₂ | M ₂ | M ₃ | M ₄ | M ₅ | | | |
| Size (μm) | 75 | 150 | 25 | 25 | 35 | | | |
| Capacitor | C ₁ | C ₂ | C ₃ | C ₄ | C ₅ | C ₆ | C ₇ | C ₈ |
| Value (pF) | 5.0 | 1.0 | 0.2 | 0.25 | 2.0 | 2.0 | 0.01 | 0.22 |
| Inductor | L ₁ | L ₂ | L ₃ | L ₄ | | | | |
| Value (nH) | 7.54 | 2.98 | 3.37 | 4.28 | | | | |
| Resistor | R ₁ | | | | | | | |
| Value (Ω) | 10 | | | | | | | |

Table 2 — Performances of the proposed UWB LNA, compared with other LNAs

| | Process | BW (GHz) | Gain _{max} (dB) | NF _{min} (dB) | IIP3 (dBm) | Power (mW) |
|---------------|---------|----------|--------------------------|------------------------|------------|------------------|
| [2]+ | 0.18 μm | 3.1-10.6 | 17.5 | 3.1 | N/A | 33.2 |
| [3]+ | 0.18 μm | 2-10.6 | 14.8 | 4.3 | -6 | 24 |
| [5]* | 0.18 μm | 2-4.6 | 9.8 | 2.3 | -7 | 12.6 |
| [6]+ | 0.18 μm | 3-7 | 15.3 | 1.4 | N/A | 15 |
| [7]+ | 0.18 μm | 3-5 | 17.2 | 2.5 | -9.7 | 15.7 |
| [9]* | 0.25 μm | 3.2-4.8 | 7.5 | 2.7 | 4 | 20 |
| [10]* | 0.13 μm | 2-4.6 | 9.5 | 3.5 | -0.8 | 16.5 |
| [11]* | 0.18 μm | 3-4.8 | 13.9 | 4.7 | 0.12 | 14.6 |
| [13]+ | 0.18 μm | 3.1-4.8 | 17 | 3.9 | N/A | 21 |
| [19]* | 0.13 μm | 3.432 | 10.5 | 4.4 | -10.3 | 3.6 [#] |
| | | 3.960 | 11.7 | 4.6 | -10.1 | 3.6 [#] |
| | | 4.488 | 10.9 | 4.8 | -11 | 3.6 [#] |
| [20]* | 0.18 μm | 3.432 | 15.4 | 2.7 | -9.4 | 11.9 |
| | | 3.960 | 15.3 | 2.7 | -9 | 11.9 |
| | | 4.488 | 16 | 2.7 | -8.8 | 11.9 |
| [22]+ | 0.18 μm | 3.1-10.6 | 11.7 | 2.9 | -10.4 | 10 |
| Present work+ | 0.18 μm | 3.432 | 15.9 | 3.4 | -7.1 | 5 |
| | | 3.960 | 17.6 | 3.3 | -9.3 | 5 |
| | | 4.488 | 16.9 | 3.3 | -8.1 | 5 |

+Simulation results

* Measurement results

only core LNA

$$K = \frac{1 - |S_{11}|^2 - |S_{22}|^2 + |\Delta|^2}{2|S_{12}S_{21}|} > 1) \quad \dots (22)$$

$$|\Delta| = |S_{11}S_{22} - S_{12}S_{21}| < 1 \quad \dots (23)$$

There are trade-offs among gain, power dissipation, and linearity. The proposed LNA can be optimized to high gain and low power consumption. Table 1 lists the sizes and values of devices and Table 2 lists the performances of the proposed band-selective UWB LNA. It is compared with other previously reported LNAs. This work provides some advantages such as sufficient gain and lower power consumption.

4 Conclusions

This paper proposed a band-selective LNA operating at the 3.432, 3.960, and 4.488 GHz frequency bands to cover the 3-5 GHz UWB band. The proposed LNA is implemented with the TSMC 0.18 μm RF CMOS process using a 1.8-V supply voltage. The

active MOS g_m -boosting technique was used to improve gain and noise figure with wide input matching and low power dissipation. The current-reuse technique, which generates common-gate and common-source amplifiers using the same bias current, can as well reduce power consumption. We proposed the novel dual input matching network without using additional devices such as inductor and active stage. Therefore, the LNA reduces die area and improves linearity and noise performances. The RC-feedback common-source buffer was also used to achieve a sufficient gain for output matching. The LNA showed simulated gains of 15.9, 17.6, and 16.9 dB, and noise figures of 3.38, 3.28, and 3.27 dB at 3.432, 3.960, and 4.488 GHz frequency bands, respectively. A switched capacitor was implemented for band selection without an additional inductor, which requires a large chip size.

It attenuated undesired interference and unnecessary noise sources. Because the proposed LNA achieves wide

input impedance matching with two resonance frequencies, the frequency interested can be changed easily as capacitance variation of switched capacitor. We optimized the LNA with high gain and low power consumption. Therefore, the UWB LNA consumed only 5 mW at 1.8 V. The simulated results of the band-selective UWB LNA outperform the conventional LNA systems in terms of high gain and low power consumption with wide tuning range.

Acknowledgement

This work was supported by the Basic Science Research Program through the National Research Foundation of Korea, funded by the Ministry of Education, Science and Technology under Grant NRF-2018R1D1A1B07042378.

References

- 1 Guan X & Nguyen C, *IEEE T Microw Theory*, 54 (2006) 3278.
- 2 Lu Y, Yeo K S, Cabuk A, Ma J, Do M A & Lu Z, *IEEE T Circuits-I*, 53 (2006) 1683.
- 3 Chen K H, Lu J H, Chen B J & Liu S I, *IEEE T Circuits- II*, 54(3) (2007) 217.
- 4 Zhan J H & Taylor S S, *A 5 GHz resistive-feedback CMOS LNA for low-cost multi-standard applications*, paper presented at IEEE International Solid-State Circuits Conference, San Francisco, US, 2006.
- 5 Kim C W, Kang M S, Anh P T, Kim H T & Lee S G, *IEEE J Solid-St Circ*, 40 (2005) 544.
- 6 Doh H, Jeong Y, Jung S & Joo Y, *Design of CMOS UWB low noise amplifier with cascade feedback*, paper presented at Midwest Symposium on Circuits and Systems, 2004.
- 7 Chen S C, Wang R L, Kung M L & Kuo H C, *An integrated CMOS low noise amplifier for 3-5 GHz UWB applications*, paper presented at IEEE Conference on Electron Devices and Solid-State Circuits, 2005.
- 8 Perumana B G, Zhan J H C, Taylor S S, Carlton B R & Laskar J, *IEEE T Microw Theory*, 56 (2008) 1218.
- 9 Lerdworatawee A J & Namgoong W, *IEEE T Circuits-I*, 52 (2005) 2327.
- 10 Bevilacqua A, Sandner C, Gerosa A & Neviani A, *IEEE Microw Wirel Co*, 16 (2006) 134.
- 11 Jeong M I, Lee J N & Lee C S, *Electron Lett*, 44 (2008) 477.
- 12 Chehraz S, Mirzaei A, Bagheri R & Abidi A A, *A 6.5 GHz wideband CMOS low noise amplifier for multi-band use*, paper presented at IEEE Custom Integrated Circuits Conference, San Jose, US, 2005.
- 13 Vishwakarma S, Jung S & Joo Y, *Ultra wideband and CMOS low noise amplifier with active input matching*, paper presented at International Workshop on Ultra Wideband Systems joint with Conference on Ultrawideband and Systems and Technologies, 2004.
- 14 Belmas F, Hameau F & Fournier J M, *IEEE J Solid-St Circ*, 47 (2012) 1094.
- 15 Shim J, Yang T & Jeong J, *Microelectron J*, 44 (2013) 821.
- 16 Khurram M & Hasan S M R, *IEEE T VLSI Syst*, 20 (2012) 400.
- 17 Shim J & Jeong J, *Microelectron J*, 65 (2017) 78.
- 18 Shim J & Jeong J, *Int J Electron*, 102 (2015) 1609.
- 19 Fu C T, Ko C L, Kuo C N & Juang Y Z, *IEEE T Microw Theory*, 56 (2008) 2754.
- 20 Tang S K, Pun K P, Choy C S, Chan C F & Leung K N, *IEEE T Circuits- II*, 55 (2008) 653.
- 21 Kim B, Kim D & Nam S, *J Electromagn Eng Sci*, 14 (2014) 47.
- 22 Hsu M T, Chang Y C & Huang Y Z, *Microelectron J*, 44 (2013) 1223.
- 23 Walling J S, Shekhar S, Allstot D J, *A g_m -boosted current-reuse LNA in 0.18 μm CMOS*, paper presented at IEEE Radio Frequency Integrated Circuits Symposium, Honolulu, US, 2007.
- 24 Chamas I R & Raman S, *IEEE T Microw Theory*, 57 (2009) 542.
- 25 Lin Y S, Chen C Z, Yang H Y, Chen C C, Lee J H, Huang G W & Lu S S, *IEEE T Microw Theory*, 58 (2010) 287.
- 26 Martins M A, Fernandes J R & Silva M M, *Techniques for dual-band LNA design using cascade switching and inductor magnetic coupling*, paper presented at IEEE International Symposium on Circuits and Systems, New Orleans, US, 2007.
- 27 Toofan S, Rahmati A R, Abrishamifar A & Roientan L G, *Microelectron J*, 39 (2008) 1534.
- 28 Gonzalez G, *Microwave Transistor Amplifiers: Analysis and Design. 2nd ed.* (Prentice-Hall, New Jersey), 1997.